



Warburg's method as a simple tool for measuring oxygen uptake in spray-dried emulsions



Bruna Barbon Paulo^{a,*}, Fernando Divino de Oliveira Júnior^a, Izabela Dutra Alvim^b, Ana Silvia Prata^a

^a Department of Food Engineering, School of Food Engineering, State University of Campinas (UNICAMP), 80 Monteiro Lobato St., CEP: 13083-862, Campinas, SP, Brazil

^b Institute of Food Technology (ITAL), Center for Technology of Cereals and Chocolates, 2880 Brasil Ave., CEP: 13070-178, Campinas, SP, Brazil

ARTICLE INFO

Keywords:

Oxidative stability
Microencapsulation
Spray drying
Warburg's method

ABSTRACT

Lipid oxidation is usually responsible for oil downgrading of spray-dried powders and it is strongly dependent on the storage conditions. Direct measurements of the oxygen uptake using cost-effective methods combined with the study of water adsorption of the powders allow evaluating their barrier properties against oxidation. Therefore, a low-cost and simple apparatus based on the Warburg's manometric technique was built, and its results were compared to Rancimat and Oxipres methods. Firstly, free unsaturated oil (fish oil) was evaluated and data showed a strong positive correlation between the oxygen uptakes for the new apparatus (0.015 mL O₂/h) and Oxipres method (Pearson's coefficient = 0.97). After, different surface-active compounds (SAC) (whey protein isolate – WPI, gelatin – GE, or modified starch – MS) mixed to maltodextrin (MD) were used to encapsulate the fish oil via spray drying. The lowest oxygen uptake was obtained by MD + WPI (0.0018 mL O₂/h), followed by MD + GE (0.0103 mL O₂/h) and MD + MS (0.0291 mL O₂/h), with similar behavior obtained by Rancimat method. The lowest protective barrier of MD + MS-powders was confirmed by the comparatively higher susceptibility to water adsorption, and consequently the lower glass transition temperature (~58.7 °C at water activity = 0.3–0.4). This study presented a successful creation of an apparatus to provide useful, fast and effective information about oxygen consumption by fish oil and encapsulated fish oil, allowing the understanding of the protection of SAC against oxidation in spray-dried emulsions. The proposed apparatus can be easily implemented in laboratories, with potential application for other oxygen-sensitive products.

1. Introduction

Unsaturated triglycerides, such as algal, fish, flaxseed, chia, are important for human health due to their nutritional value, but they are highly susceptible to degradation reactions. Lipid oxidation is one of the main leaders of oil downgrading and microencapsulation is usually an effective way to incorporate these oils in formulations. It provides a protective layer around the oil, preserving its sensory quality and nutritional value, and then, increasing its shelf life (Anwar & Kunz, 2011; Encina, Vergara, Giménez, Oyarzún-Ampuero, & Robert, 2016; Keogh et al., 2001).

Among the different techniques of microencapsulation, spray drying produces powders with low moisture and water activity, allowing long-term storage and reduced transport costs. Thus, the spray drying of oil-in-water emulsions has been successfully applied for the protection of unsaturated oils against oxidation (Carneiro, Tonon, Grosso, & Hubinger, 2013; Noello, Carvalho, Silva, & Hubinger, 2016; Silva,

Azevedo, Cunha, Hubinger, & Meireles, 2016). Such protection has been evaluated through the oxidative stability by quantifying the level of peroxides (Drusch, Serfert, Van Den Heuvel, & Schwarz, 2006; Drusch, 2007; Wang, Liu, Dong, & Selomulya, 2016), secondary compounds (Charve & Reineccius, 2009; Drusch et al., 2006; Drusch, 2007), or measuring the conductivity using Rancimat method (Giorgio, Salgado, & Mauri, 2019; Hoyos-Leyva, Bello-Perez, Agama-Acevedo, & Alvarez-Ramirez, 2019; Velasco, Dobarganes, Holgado, & Márquez-rui, 2009; Vishnu et al., 2017; Wang, Adhikari, Mathesh, Yang, & Barrow, 2019). However, these analytical techniques may present complexity, due to the possibility of chemical reactions between the components during the analysis, the previous extraction of the inner oil may cause further oxidation, and, for the Rancimat method, the active compound may be oxidizing inside the matrix without the necessary release of the degradation compounds for changing the conductivity measurement.

In this context, the estimation of the rate of oxygen crossing the

* Corresponding author.

E-mail address: brunabarbonpaulo@gmail.com (B. Barbon Paulo).

polymeric barrier combined with the evaluation of physicochemical properties of the particles can supply strategic guidelines for the understanding of how the structured matrices can limit oxidation reactions. A method, called Warburg's manometric technique, allows to quantify the volume of consumed oxygen by measuring the changes of the pressure in a hermetically closed recipient containing the samples. In the literature, there are works since the 1940s for application of this method for the estimation of respiration rate of living organisms (Perkins, 1943; Umbreit, Burris, & Stauffer, 1972), but few studies applied it for evaluating the oxidation reactions, as freeze-dried (Gejl-Hansen & Flink, 1977; Maloney, Labuza, Wallace, & Karel, 1966; Martinez & Labuza, 1968) and spray-dried products (Anandaraman & Reineccius, 1986). Based on the same principle, the Oxipres has been applied to estimate the shelf life of food products (Polavarapu, Oliver, Ajlouni, & Augustin, 2011; Wang, Adhikari, & Barrow, 2019; Wang, Adhikari, Barrow et al., 2019; Wang, Adhikari, Mathesh et al., 2019), but it is a high-cost and rarely used equipment. Therefore, this study aimed to revisit Warburg's technique by building a simple and low-cost apparatus to obtain direct measurements of oxygen consumption of spray-dried powders over 48 h. The second objective was to evaluate the effectiveness of different polymeric matrices to protect unsaturated triglycerides against oxidation. From this study, the understanding of the food-structure function relationships of spray-dried powders was supported through physicochemical characterization and behavior of the water adsorption.

2. Material and methods

2.1. Material

Fish oil (FO) (Incromega E3322-LQ-(LK), Croda Europe Ltd., United Kingdom) composed by 33 % (w/w) of eicosapentaenoic acid (EPA) and 22 % (w/w) of docosahexaenoic acid (DHA) was used as the active compound. Maltodextrin (MD) (MOR-REX® 1910, dextrose equivalent (DE) = 10, Ingredion Brasil Ingredientes Ltda, Mogi Guaçu, Brazil), modified starch (MS) (Capsul®, Ingredion Brasil Ingredientes Ltda, Mogi Guaçu, Brazil), gelatin (GE) (100 H 30, Rousselot Gelatinas do Brasil Ltda, Amparo, Brazil) and whey protein isolate (WPI) (Fonterra Ltd., Tokoroa, New Zealand) were employed to compose the wall materials.

2.2. Production of the particles

Emulsions (30 % w/w total solids) with FO (6 % w/w) and three different matrices: MD (22.8 % w/w) and MS (1.2 % w/w) (MD + MS), or MD (22.8 % w/w) and WPI (1.2 % w/w) (MD + WPI), or MD (20.4 % w/w) and GE (3.6 % w/w) (MD + GE) were produced. This ratio of the surface-active compound and MD was selected based on the better emulsions' stability obtained by Paulo, Alvim, Reineccius, & Prata, 2020. The ratio of the oil to wall material was maintained at 1:4, which means that the final composition of all dried particles was 20 % oil and 80 % of the wall material (dry basis) (Charve & Reineccius, 2009; Jafari, Assadpoor, Bhandari, & He, 2008; Jafari, Assadpoor, He, & Bhandari, 2008). The FO was emulsified at 11,200 rpm for 90 s using an Ultra-Turrax mixer (T18BS1, IKA T18 basic, Germany). The emulsions (droplet mean size $\approx 2.0 \mu\text{m}$ for MD + MS and WPI + MS-emulsions and $10 \mu\text{m}$ for MD + GE-emulsions (Paulo et al., 2020)) were atomized through a dual fluid atomizer nozzle (Inner Diameter I.D. 0.7 mm) at the feed rate of 0.8 L/h and dried using a spray dryer (B-290, Büchi, Flawil, Switzerland). The experimental tests were performed in duplicate with the inlet and outlet air drying temperature of 180 °C and 90 °C, respectively.

2.2.1. Measurement of oxidative stability

2.2.1.1. Oxygen uptake: apparatus based on Warburg's methodology. A lab-scale apparatus was built based on Warburg's methodology (Perkins, 1943) and it consists in a system formed by an amber glass

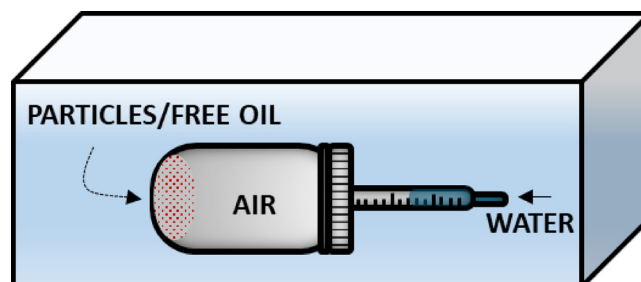


Fig. 1. New apparatus by Warburg's method.

flask (20 mL, $D = 3 \text{ cm}$; $L = 3 \text{ cm}$), in which a syringe (100 U.I., outer diameter O.D. = 0.4 cm, $L = 8 \text{ cm}$) with a millimetric scale (0.01 mL) is coupled (Fig. 1). The flask containing the sample is immersed in a water bath, which was used as the manometric fluid. Initially, water enters into the capillary until equilibrium (initial manometric pressure). There is no additional differential pressure between the systems at a lower pressure (flask) and upper pressure (water bath), preventing the further entrance of liquid. When the oil oxidation process starts, the consumption of the oxygen makes the water enters into the syringe, moving the meniscus as a function of the time.

For the experimental tests, a certain amount of FO or particles (1.0 g) was weighed and added inside the flask of the new apparatus and the respective readings of the water in the meniscus were done periodically over 48 h. The slope of the oxygen uptake (mL O_2) versus time (h) was used for determining the oxygen consumption rate ($\text{mL O}_2/\text{h}$).

In order to avoid the effects of variation of the volume of the inner air, an empty flask was used as control. Particularly for particles' experiments, the control was the flasks with the spray-dried wall materials without oil to eliminate the water absorption effect, since the wall materials (MD + WPI, MD + GE or MD + MS) are highly hygroscopic (Bustamante, Masson, Velasco, Manuel, & Robert, 2016; da Silva et al., 2013; Santiago et al., 2016). Thus, the oxygen uptake of the encapsulated oil was calculated by the difference between values measured for the particles and the wall materials.

Besides, an evaluation of the amount of the mass of the sample and its relation with the exposed area was done using different amounts of free FO (1.0 and 0.1 g). Thus, an index (I_{AV}) that measures this relation between the exposed area of the oil and headspace volume of the apparatus was determined as follows in Eq. (1):

$$I_{AV} = \frac{\frac{\pi D^2}{4}}{V_{flask} - V_{sample}} \quad (1)$$

Where D is the diameter of the flask, V_{flask} is the total volume of the flask and V_{sample} is the volume occupied by the sample.

2.2.1.2. Oxygen uptake: oxygen bomb methodology. Oxipres apparatus (Mikrolab Aarhus A/S, Højbjerg, Denmark) measures the pressure inside of a hermetically closed iron vessel at a controlled temperature. Twenty g of bulk FO was added in a cylindrical vessel (125 mL, height = 10 cm; diameter = 5 cm) and the system was maintained at room temperature ($\sim 25 \text{ }^\circ\text{C}$) and atmospheric pressure ($\sim 1 \text{ bar}$) for 48 h, which are the same conditions adopted in Warburg's method. The results given by the equipment are expressed in pressure difference (ΔP) and they were converted to the volume of consumed oxygen, as follows in Eqs. (2) and (3).

$$\Delta n = \frac{\Delta P V}{R T} \quad (2)$$

$$V_{O_2} = \frac{\Delta n M M}{\rho_{O_2}} \quad (3)$$

Where Δn is the variation of the number of moles (consumed O_2 mol), ΔP is the pressure difference (N/m^2), R is the gas constant (8.314 J/mol)

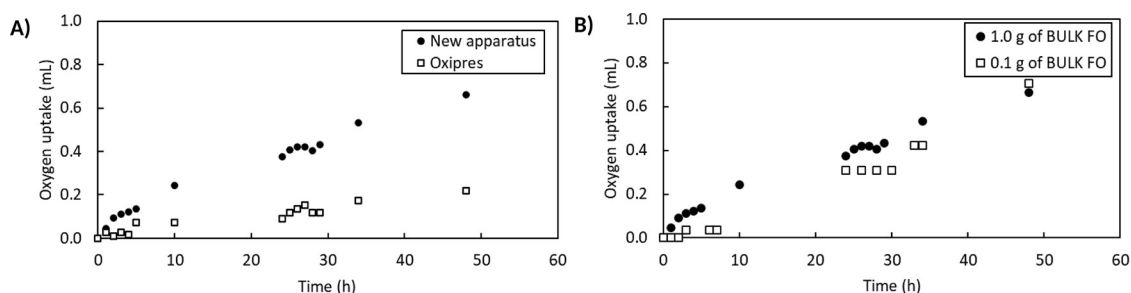


Fig. 2. Oxygen uptake for the free oil at room temperature for 48 h: a) Warburg's apparatus and Oxipres equipment; b) Warburg's apparatus containing two different amounts of free fish oil.

K), T is the temperature ($25\text{ }^{\circ}\text{C} = 278\text{ K}$) and V is the free volume in the iron vessel (75.91 cm^3 for oil), which is given by the difference between the total volume (125 cm^3) and the volume occupied by the sample (49.09 cm^3 for oil), V_{O_2} is the consumed O_2 volume (cm^3), MM is the molar mass (32 g/mol), ρ_{O_2} is the O_2 density (1.33 g/cm^3)

The index (I_{AV}) was also measured for Oxipres methodology according to Eq. (1).

2.2.1.3. Rancimat method. The particle oxidation was evaluated indirectly by the Rancimat method, in which the volatile oxidation products are monitored according to the induction time measured by the conductivity provided by oxidation products formed. The system allows evaluating the induction period of the curve $K = f(t)$, where K is the conductivity expressed as $\mu\text{S/cm}$ and the time in hours (t). Induction time is defined by the time required to reach the inflection point in the curve, which is calculated by the intersection of the line tangent to the curve projected along the time axis. The induction time was measured by the Biodiesel Rancimat 873 (Metrohm, Herisau, Switzerland) with a 2.0 g sample, heated to $120\text{ }^{\circ}\text{C}$, under a purified airflow rate of 20 L/h , in duplicate.

2.2.2. Sorption isotherms

Sorption isotherms were determined for FO-particles by the gravimetric method according to Mortenson, Labuza, and Reineccius (2010), with some modifications. Duplicate samples of approximately 0.5 g were carefully weighed and placed in recipients containing the following over saturated salt solutions (a_w): lithium chloride (0.113); magnesium chloride (0.328); potassium carbonate (0.432); magnesium nitrate (0.529); potassium iodide (0.689); sodium chloride (0.753); potassium chloride (0.843) (Labuza, 1984). The samples were stored in an incubator at $25\text{ }^{\circ}\text{C}$ and they were weighed every 2 days for 3 weeks until reaching the equilibrium. Data from the initial moisture content data were used to construct "working" isotherms. Isotherms were plotted using the equilibrium moisture contents of the products and the BET and GAB models were adjusted to the data (Van Den Berg & Bruin, 1981). The GAB model (Eq. (4)) obtained the most suitable adjustment, based on the high coefficient of determination (R^2), and therefore, it was used to discuss the results. The low mean relative percentage deviation modulus (E) was also calculated as follows in Eq. (5).

$$X_{eq} = \frac{X_m C K a_w}{(1 - K a_w)(1 - K a_w + C K a_w)} \quad (4)$$

where X_{eq} : equilibrium moisture content ($\text{g H}_2\text{O g}^{-1}$ dry powder); X_m : monolayer moisture content ($\text{g H}_2\text{O g}^{-1}$ dry powder); C , K : model constants related to the monolayer and monolayer properties; a_w : water activity.

$$E = \frac{100}{N} \sum_{i=1}^N \frac{|m_i - m_{pi}|}{m_i} \quad (5)$$

where m_i is the experimental value, m_{pi} is the predicted value and N is the population of experimental data.

2.2.3. Glass transition temperature

FO-samples equilibrated at a_w of 0.3–0.4 were weighed (6–7 mg) and sealed hermetically in aluminum pans. Heating and cooling cycles were performed at $10\text{ }^{\circ}\text{C/min}$ rate using a differential scanning calorimetry (DSC) (DSC 250, TA Instruments, New Castle, USA) as follows: heating from $25\text{ }^{\circ}\text{C}$ to $160\text{ }^{\circ}\text{C}$, 5 min at $160\text{ }^{\circ}\text{C}$, cooling from $160\text{ }^{\circ}\text{C}$ to $25\text{ }^{\circ}\text{C}$, 15 min at $25\text{ }^{\circ}\text{C}$. The thermograms obtained were normalized based on the mass of the samples. All analyses were done in duplicate and the data were treated by the software TA Instruments Trios (TA Instruments, New Castle, USA).

2.2.4. Fourier Transform Infrared Spectroscopy (FTIR)

Samples were ground with KBr and compressed by a hydraulic press, forming pellets that were used in a FTIR spectrometer (IRPrestige-21, Shimadzu, Kyoto, Japan). Samples were analyzed in the $4000\text{--}400\text{ cm}^{-1}$ regions, with a resolution of 4 cm^{-1} for 100 scans.

2.2.5. X-ray diffractometry

The X-ray diffraction analysis of the wall materials and spray-dried particles was performed on a Philips Analytical X-Ray (X'Pert-MPD, Almelo, Netherlands) using a graphite crystal monochromator with $\text{Cu-K}\alpha_1$ filter radiation of $\lambda = 1.5406\text{ \AA}$ at 40 kV and 40 mA. The samples were analyzed in angles from 5° to 50° (2θ) with a step of 0.02° ($1.2^{\circ}/\text{min}$).

3. Results and discussion

The results of oxygen uptake for the free oil obtained with Warburg's apparatus and Oxipres at room temperature over 48 h are shown in Fig. 2A.

The oxygen uptake for the FO was crescent over time with a strong positive correlation between the two methodologies, i.e., Pearson's coefficient between the oxygen uptakes determined by the new apparatus and Oxipres method corresponded to 0.97. The rate of the oxygen consumption obtained by Warburg's apparatus ($0.015\text{ mL O}_2/\text{h}$) was higher in comparison to Oxipres equipment ($0.0045\text{ mL O}_2/\text{h}$). These results can be explained for the differences in the exposed area of the oxygen for the two methods. The relation between the surface area of the oil and headspace volume available was calculated for both methodologies through an index (I_{AV}). The Warburg's apparatus presented a higher index ($I_{AV} = 33.33\text{ m}^{-1}$) in comparison with Oxipres technique ($I_{AV} = 25.86\text{ m}^{-1}$), which means that for the same amount of available oxygen, the samples in the Warburg's apparatus have a higher exposed area to oxidation reaction to occur. The high exposed area of Warburg's apparatus was confirmed when the effects of the amount of the sample on the oxygen uptake were evaluated (Fig. 2B). The oxygen consumption showed similar behavior for the two different amounts of FO, being the index I_{AV} corresponding to 33.33 and 32.05 m^{-1} for 1.0 and 0.1 g, respectively. This result showed that the amount of sample did not affect significantly the oxidation reaction behavior, because the relation between the exposed area of the oil to oxidation reaction and the headspace volume was kept constant. Additionally, the higher relative

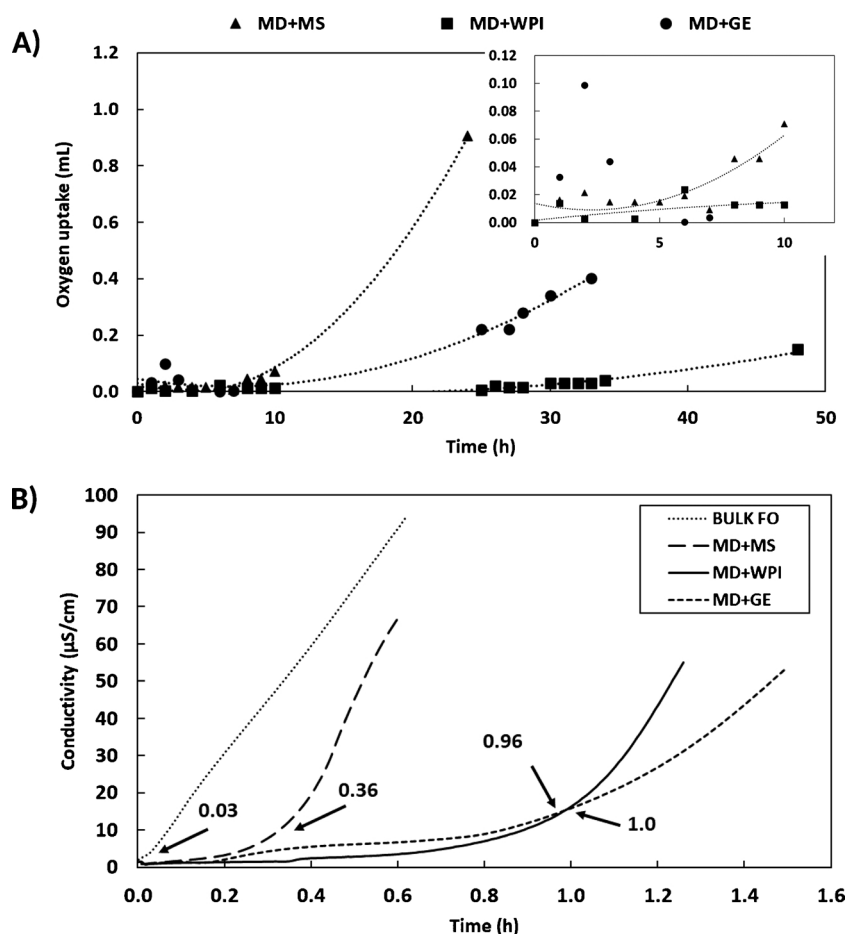


Fig. 3. Oxygen uptake of the encapsulated fish oil: a) New the apparatus at room temperature for 48 h; b) Accelerated oxidative stability test using Rancimat at 120 °C and O₂ flow rate of 20 L/h.

humidity in the Warburg's apparatus may have also contributed to further increase the oxidation (Fennema, Damodaran, & Parkin, 2017), since water content is considered a major factor affecting the rate of lipid oxidation in food matrices (Labuza, McNally, Gallagher, Hawkes, & Hurtado, 1972).

Thus, Warburg's apparatus was applied to evaluate the performance of the wall materials for protecting the FO against oxidation. These results are shown in Fig. 3A. In order to compare the performance of the matrices obtained by Warburg's method, the oxidation stability was analyzed in the equipment Rancimat (Fig. 3B).

Both methods showed that particles containing proteins as wall materials (MD + WPI and MD + GE) provided a higher protective effect against oxidation of the oil. Similar to this work, Carneiro et al. (2013) and Charve and Reineccius (2009) also found that the presence of proteins as wall materials showed a higher capacity for limiting oxidation reaction than modified starches (Hi-Cap and/or Capsul). Once the new apparatus showed consistent results for both bulk oil and particles in comparison to the two techniques (Oxipres and Rancimat), this study can provide new insights about its building, allowing to enlarge its application for other encapsulated oxygen-sensitive compounds.

Specifically, in the Rancimat's method, the change of the conductivity of the water is due to the release of the compounds from the oxidation, and thus, the oxidative stability is related to the induction time values. The free FO presented a very short induction time of 0.03 h (Fig. 3B), proving its high susceptibility to oxidation. As expected, the encapsulated oil showed oxidative stability higher at least 12 times, being the highest induction time obtained for the MD + GE (1 h), followed by MD + WPI (0.96 h) and MD + MS (0.36 h) matrices. For

Warburg's method, MD + WPI presented the lowest oxygen uptake rate (0.0018 mL O₂/h), followed by MD + GE (0.0103 mL O₂/h) and MD + MS (0.0291 mL O₂/h). The magnitude order of these values are similar to those ones obtained in earlier studies using the Warburg's methodology for spray-dried powders with orange peel oil and gum Arabic (Anandaraman & Reineccius, 1986), and freeze-dried emulsions containing fatty acids (Gejl-Hansen & Flink, 1977; Maloney et al., 1966).

However, MD + MS particles showed a higher oxygen uptake rate than free oil in the Warburg's apparatus. The particles present a higher surface area than the free and bulk FO, which can cause a higher oxygen uptake measured by the Warburg's method. Polavarapu et al. (2011), Wang, Adhikari, Barrow et al. (2019), and Wang, Adhikari, Mathesh et al. (2019) also showed that the comparison between the powdered samples and the bulk unsaturated oil using Oxipres method is not possible due to the differences of the exposed area to the oxygen, confirming that the new apparatus performed as expected.

Trying to relate the thermodynamic state of the water in the food powders to their physicochemical stability, the study of sorption isotherms was carried out for all particles (Fig. 4) and the GAB model was adjusted to the experimental data. Table 1 summarizes the sorption constants C , K and X_m (monolayer value) obtained for the GAB model, which was the better adjustment for all particles ($R^2 > 0.9$) with $K < 1$.

The moisture sorption isotherms at 25 °C for all samples were sigmoidal type, which is expected for products containing polymeric ingredients, like proteins and polysaccharides (Fennema et al., 2017). The x-ray diffractogram patterns (Fig. 5A) showed a characteristic broad peak of molecular disorder for all powders, which is indicative of the amorphous state (Fennema et al., 2017), corroborating to the results obtained for sorption isotherms.

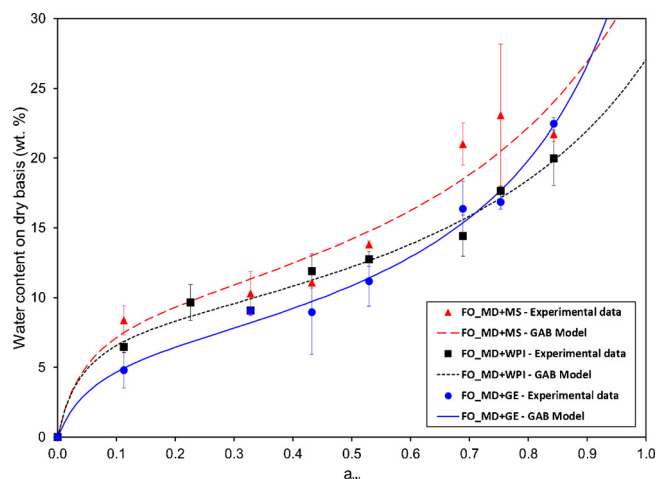


Fig. 4. Sorption isotherms for fish oil particles with matrices containing MD + MS, MD + WPI, or MD + GE.

Table 1

Sorption isotherms for fish oil particles: a) maltodextrin + modified starch; b) maltodextrin + whey protein isolate; c) maltodextrin + gelatin.

Samples	K	C	X_m	E (%)	R^2
MD + MS	0.72	28.04	0.097	24.66	0.89
MD + WPI	0.69	35.84	0.084	3.97	0.95
MD + GE	0.83	18.50	0.068	3.04	0.99

K , C : model constants related to the monolayer; X_m : monolayer moisture content ($\text{g H}_2\text{O g}^{-1}$ dry powder); E : mean relative percentage deviation modulus (%).

The similar sigmoidal behavior and the amorphous state can be due to the maltodextrin being the majority component for all powders, but slight differences were observed for the behavior of water adsorption and glass transition temperatures. The results demonstrated a tendency

to MD + MS-powders show the highest monolayer moisture content ($X_m = 0.097$), which means they appear to be more hygroscopic than protein powders. Fig. 4 showed a higher amount of hydrated chemistry groups for MD + MS-powders, specifically when the water activity is increased from 0.2 to 0.7. MD + MS particles presented a tendency to present lower glass transition temperature (58.7°C) than MD + WPI (61.9°C) and MD + GE (68.1°C) at water activity ranging from 0.3 to 0.4, indicating the higher susceptibility of MD + MS sample to destabilization under certain conditions of storage.

According to Escalona-García et al. (2016), the differences in the physical stability between the matrices can be attributed to a combination of factors, which include the conformation and topology of the molecule and the hydrophilic/hydrophobic sites adsorbed at the interface. Fig. 5B shows the Fourier Transform Infrared Spectroscopy (FTIR) spectral absorption bands of the wall materials (MS, WPI, GE, MD) and the FO particles, highlighting the possible changes associated with the wall material.

All powders showed a profile similar to the pure MD and this was expected as it is the major component of the sample. Also, some distinctions were verified because of the presence of the oil. The FO exhibited a band at 1744 cm^{-1} (C=O stretch from lipids) and a triplet band at the range of $2800\text{--}3000\text{ cm}^{-1}$, which represents the C–H bonds of methyl and methylene of fatty acids (Vongsivut et al., 2012). Slight changes were observed due to the proteins or modified starch, as they were present in very low concentrations in the samples. Comparing the three types of spray-dried powders, a notable difference is in the peak at 1540 cm^{-1} , highlighted in the Fig. 5B, which represents the N–H bonds and stretching vibrations of the C–N group and C–C (Bouyanfif, Liyanage, Hequet, Moustaid-Moussa, & Abidi, 2019). The MD + MS particles present a monomodal peak in that wavelength, as MD + WPI and MD + GE particles showed a bimodal behavior. This peak could have occurred because the proteins are mostly composed of amino acid groups, which increases the C–N and N–H interactions of the sample and that promotes a second peak at the 1540 cm^{-1} range. Likewise, in MD + MS samples the C–C bond prevails, causing only one band in that wavelength. Moreover, the particle spectra exhibit peaks at 1744 cm^{-1} and the triplet band in the range of $2800\text{--}3000$

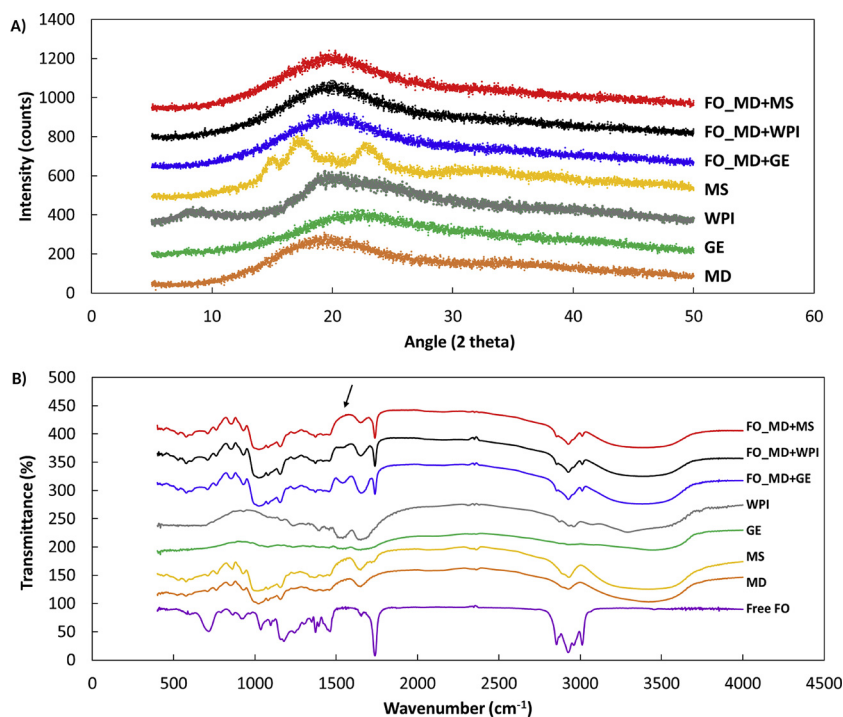


Fig. 5. Physical characteristics of the raw wall materials (modified starch, whey protein isolate, gelatin, and maltodextrin) and the fish oil particles (maltodextrin + modified starch, maltodextrin + whey protein isolate, maltodextrin + gelatin): a) X-ray diffraction patterns; b) FTIR spectra.

cm^{-1} , which implies the presence of oil in the microcapsules (Vongsivut et al., 2012). Moreover, there were no changes in the characteristic bands of the particles in comparison with the raw materials, therefore it is concluded that the spray drying process causes no chemical interactions between the wall components and the active compound (Kutzli, Gibis, Baier, & Weiss, 2019).

4. Conclusions

A very simple and low-cost apparatus based on Warburg's method was developed and it could be applied properly for quantifying the oxygen uptake in unsaturated triglycerides and encapsulated food powders. The results were compared to the Oxipres methodology and presented a strong correlation between both methods (Pearson's coefficient = 0.97) using free unsaturated oil (FO), which presented an oxygen uptake of 0.015 mL O_2/h . The oxidation stability of spray-dried FO powders with matrices containing very low levels of MS, WPI and GE was compared to Rancimat method. Both methods presented similar behavior for all particles, showing the new apparatus was properly developed. The lowest oxygen uptake was obtained by MD + WPI matrix, followed by MD + GE and MD + MS, whose rates were 0.0018, 0.0103 and 0.0291 mL O_2/h for the encapsulated oil, respectively. In order to support the results of oxygen uptake, the behavior of water adsorption was studied. All powders were composed mostly by maltodextrin, resulting very similar FTIR spectra, X-ray diffraction patterns and similar sigmoidal sorption isotherm at 25 °C. However, slight differences were observed for MD + MS-particles that presented a tendency to higher susceptibility to water adsorption ($X_m = 0.097$) and lower glass transition temperature (~ 58.7 °C at water activity = 0.3–0.4). This result could support its low protective barrier showed by the new apparatus, which leads to the highest oxygen uptake. The data obtained suggested that the apparatus can be used to indicate the degree of oxidation of both free and encapsulated oxidable oils.

This study allowed a successful building of an apparatus based on Warburg's technique to evaluate the oxidation in oxygen-sensitive products and, consequently, enlarging the range of cost-effective methods.

Acknowledgements

The authors gratefully acknowledge the FAPESP for the financial support [grant numbers 2017/14271-7 and 2017/15410-0], the Croda Europe Ltda, Ingredion Brasil Ingredientes Ltda, Fonterra Ltda and Rousselot Gelatinas do Brasil Ltda for the donation of the materials.

References

- Anandaraman, S., & Reineccius, G. A. (1986). Stability of encapsulated orange peel oil. *Food Technology*, 40(11), 88–93.
- Anwar, S. H., & Kunz, B. (2011). The influence of drying methods on the stabilization of fish oil microcapsules: Comparison of spray granulation, spray drying, and freeze drying. *Journal of Food Engineering*, 105(2), 367–378. <https://doi.org/10.1016/j.jfoodeng.2011.02.047>.
- Bouyanfif, A., Liyanage, S., Hequet, E., Moustaid-Moussa, N., & Abidi, N. (2019). FTIR microspectroscopy reveals fatty acid-induced biochemical changes in *C. elegans*. *Vibrational Spectroscopy*, 102(January), 8–15. <https://doi.org/10.1016/j.vibspec.2019.03.002>.
- Bustamante, A., Masson, L., Velasco, J., Manuel, J., & Robert, P. (2016). Microencapsulation of H. vulgialis oleoresins with different fatty acid composition: Kinetic stability of astaxanthin and alpha-tocopherol. *Food Chemistry*, 190, 1013–1021. <https://doi.org/10.1016/j.foodchem.2015.06.062>.
- Carneiro, H. C. F., Tonon, R. V., Grosso, C. R. F., & Hubinger, M. D. (2013). Encapsulation efficiency and oxidative stability of flaxseed oil microencapsulated by spray drying using different combinations of wall materials. *Journal of Food Engineering*, 115(4), 443–451. <https://doi.org/10.1016/j.jfoodeng.2012.03.033>.
- Charve, J., & Reineccius, G. A. (2009). Encapsulation performance of proteins and traditional materials for spray dried flavors. *Journal of Agricultural and Food Chemistry*, 57, 2486–2492.
- da Silva, F. C., da Fonseca, C. R., de Alencar, S. M., Thomazini, M., de C. Baliero, J. C., Pittia, P., ... Fávoro-Trindade, C. S. (2013). Assessment of production efficiency, physicochemical properties and storage stability of spray-dried propolis, a natural food additive, using gum Arabic and OSA starch-based carrier systems. *Food and Bioprocess Technology*, 91(1), 28–36. <https://doi.org/10.1016/j.fbp.2012.08.006>.
- Drusch, S. (2007). Sugar beet pectin: A novel emulsifying wall component for microencapsulation of lipophilic food ingredients by spray-drying. *Food Hydrocolloids*, 21(7), 1223–1228. <https://doi.org/10.1016/j.foodhyd.2006.08.007>.
- Drusch, S., Serfert, Y., Van Den Heuvel, A., & Schwarz, K. (2006). Physicochemical characterization and oxidative stability of fish oil encapsulated in an amorphous matrix containing trehalose. *Food Research International*, 39, 807–815. <https://doi.org/10.1016/j.foodres.2006.03.003>.
- Encina, C., Vergara, C., Giménez, B., Oyarzún-Ampuero, F., & Robert, P. (2016). Conventional spray-drying and future trends for the microencapsulation of fish oil. *Trends in Food Science & Technology*, 56, 46–60. <https://doi.org/10.1016/j.tifs.2016.07.014>.
- Escalona-García, L. A., Pedroza-Islas, R., Natividad, R., Rodríguez-Huezo, M. E., Carrillo-Navas, H., & Pérez-Alonso, C. (2016). Oxidation kinetics and thermodynamic analysis of chia oil microencapsulated in a whey protein concentrate-polysaccharide matrix. *Journal of Food Engineering*, 175, 93–103. <https://doi.org/10.1016/j.jfoodeng.2015.12.009>.
- Fennema, O. R., Damodaran, S., & Parkin, K. L. (2017). In S. Damodaran, & K. L. Parkin (Eds.), *Fennema's food chemistry* (5th ed.). Boca Raton: Taylor & Francis Group.
- Gejl-Hansen, F., & Flink, J. M. (1977). Freeze-dried carbohydrate containing oil-in-water emulsions: Microstructure and fat distribution. *Journal of Food Science*, 42(4), 1049–1055.
- Giorgio, L., Di Salgado, P. R., & Mauri, A. N. (2019). Encapsulation of fish oil in soybean protein particles by emulsification and spray drying. *Food Hydrocolloids*, 87(September 2018), 891–901. <https://doi.org/10.1016/j.foodhyd.2018.09.024>.
- Hoyos-Leyva, J. D., Bello-Perez, L. A., Agama-Acevedo, J. E., & Alvarez-Ramirez, J. (2019). Characterization of spray drying microencapsulation of almond oil into taro starch spherical aggregates. *LWT – Food Science and Technology*, 101(54), 526–533. <https://doi.org/10.1016/j.lwt.2018.11.079>.
- Jafari, S. M., Assadpoor, E., Bhandari, B., & He, Y. (2008). Nano-particle encapsulation of fish oil by spray drying. *Food Research International*, 41(2), 172–183. <https://doi.org/10.1016/j.foodres.2007.11.002>.
- Jafari, S. M., Assadpoor, E., He, Y., & Bhandari, B. (2008). Encapsulation efficiency of food flavours and oils during spray drying. *Drying Technology*, 26, 816–835. <https://doi.org/10.1080/07373930802135972>.
- Keogh, M. K., O'Kennedy, B. T., Kelly, J., Auty, M. A., Kelly, P. M., Fureby, A., ... Haahr, A. M. (2001). Stability to oxidation of spray-dried fish oil powder microencapsulated using milk ingredients. *Journal of Food Science*, 66(2), 217–224. <https://doi.org/10.1111/j.1365-2621.2001.tb11320.x>.
- Kutzli, I., Gibis, M., Baier, S. K., & Weiss, J. (2019). Electrospinning of whey and soy protein mixed with maltodextrin – Influence of protein type and ratio on the production and morphology of fibers. *Food Hydrocolloids*, 93(January), 206–214. <https://doi.org/10.1016/j.foodhyd.2019.02.028>.
- Labuza, T. P. (1984). *Moisture sorption: Practical aspects of isotherm measurement and use* (2nd ed.). St. Paul: American Association of Cereal Chemists.
- Labuza, T. P., McNally, L., Gallagher, D., Hawkes, J., & Hurtado, F. (1972). Stability of intermediate moisture foods. *Journal of Food Science*, 37, 154–159.
- Maloney, J. F., Labuza, T. P., Wallace, D. H., & Karel, M. (1966). Autooxidation of methyl linoleate in freeze-dried model systems. I. Effect of water on the autocatalyzed oxidation. *Journal of Food Science*, 31(6), 878–884. <https://doi.org/10.1111/j.1365-2621.1966.tb03264.x>.
- Martinez, F., & Labuza, T. P. (1968). Rate of deterioration of freeze-dried salmon as a function of relative humidity. *Journal of Food Science*, 33(3), 241–247. <https://doi.org/10.1111/j.1365-2621.1968.tb01358.x>.
- Mortenson, M. A., Labuza, T. P., & Reineccius, G. A. (2010). Moisture sorption isotherms for un-modified and osan-substituted dextrin and gum acacia used as carrier materials for spray dried encapsulation of flavoring materials. *International Journal of Food Properties*, 13(5), 992–1001. <https://doi.org/10.1080/10942910902930643>.
- Noello, C., Carvalho, A. G. S., Silva, V. M., & Hubinger, M. D. (2016). Spray dried microparticles of chia oil using emulsion stabilized by whey protein concentrate and pectin by electrostatic deposition. *Food Research International*, 89, 549–557. <https://doi.org/10.1016/j.foodres.2016.09.003>.
- Paulo, B. B., Alvim, I. D., Reineccius, G., & Prata, A. S. (2020). Performance of oil-in-water emulsions stabilized by different types of surface-active components. *Colloids and Surfaces B: Biointerfaces*, 190(January), 110939. <https://doi.org/10.1016/j.colsurfb.2020.110939>.
- Perkins, J. J. (1943). Barcroft-Warburg manometric apparatus usage, recent developments, and applications. *Industrial and Engineering Chemistry - Analytical Edition*, 15(1), 61–68. <https://doi.org/10.1021/i560113a026>.
- Polavarapu, S., Oliver, C. M., Ajlouni, S., & Augustin, M. A. (2011). Physicochemical characterisation and oxidative stability of fish oil and fish oil-extra virgin olive oil microencapsulated by sugar beet pectin. *Food Chemistry*, 127(4), 1694–1705. <https://doi.org/10.1016/j.foodchem.2011.02.044>.
- Santiago, M. C. P., de, A., Nogueira, R. I., Paim, D. R. S. F., Gouvêa, A. C. M. S., Godoy, R. L., de, O., Peixoto, F. M., ... deA. Freitas, S. P. (2016). Effects of encapsulating agents on anthocyanin retention in pomegranate powder obtained by the spray drying process. *LWT – Food Science and Technology*, 73, 551–556. <https://doi.org/10.1016/j.lwt.2016.06.059>.
- Silva, E. K., Azevedo, V. M., Cunha, R. L., Hubinger, M. D., & Meireles, M. A. A. (2016). Ultrasound-assisted encapsulation of annatto seed oil: Whey protein isolate versus modified starch. *Food Hydrocolloids*, 56, 71–83. <https://doi.org/10.1016/j.foodhyd.2015.12.006>.
- Umbreit, W. W., Burris, R. H., & Stauffer, J. F. (1972). Manometric and Biochemical Techniques. *The New Physiologist*, 72(05), 986–987. <https://doi.org/10.1017/S0140525X00060003>.

- Van Den Berg, C., & Bruin, S. (1981). Water activity and its estimation in food systems: Theoretical aspects. In L. B. Rockland, & G. F. Stewart (Eds.). *Water activity: Influences on food quality* (pp. 1–61). New York: Academic Press, Inc. <https://doi.org/10.1016/b978-0-12-591350-8.50007-3>.
- Velasco, J., Dobarganes, C., Holgado, F., & Márquez-ruiz, G. (2009). A follow-up oxidation study in dried microencapsulated oils under the accelerated conditions of the Rancimat test. *Food Research International*, 42(1), 56–62. <https://doi.org/10.1016/j.foodres.2008.08.012>.
- Vishnu, K. V., Chatterjee, N. S., Ajeeshkumar, K. K., Lekshmi, R. G. K., Tejal, C. S., Mathew, S., ... Ravishankar, C. N. (2017). Microencapsulation of sardine oil: Application of vanillic acid grafted chitosan as a bio-functional wall material. *Carbohydrate Polymers*, 174, 540–548. <https://doi.org/10.1016/j.carbpol.2017.06.076>.
- Vongsivut, J., Heraud, P., Zhang, W., Kralovec, J. A., McNaughton, D., & Barrow, C. J. (2012). Quantitative determination of fatty acid compositions in micro-encapsulated fish-oil supplements using Fourier transform infrared (FTIR) spectroscopy. *Food Chemistry*, 135(2), 603–609. <https://doi.org/10.1016/j.foodchem.2012.05.012>.
- Wang, Y., Liu, W., Dong, X., & Selomulya, C. (2016). Micro-encapsulation and stabilization of DHA containing fish oil in protein-based emulsion through mono-disperse droplet spray dryer. *Journal of Food Engineering*, 175, 74–84. <https://doi.org/10.1016/j.jfoodeng.2015.12.007>.
- Wang, B., Adhikari, B., & Barrow, C. J. (2019). Highly stable spray dried tuna oil powders encapsulated in double shells of whey protein isolate-agar gum and gellan gum complex coacervates. *Powder Technology*, 358, 79–86. <https://doi.org/10.1016/j.powtec.2018.07.084>.
- Wang, B., Adhikari, B., Mathesh, M., Yang, W., & Barrow, C. J. (2019). Anchovy oil microcapsule powders prepared using two-step complex coacervation between gelatin and sodium hexametaphosphate followed by spray drying. *Powder Technology*, 358, 68–78. <https://doi.org/10.1016/j.powtec.2018.07.034>.